PERGAMON

Deep-Sea Research II 48 (2001) 1263–1283

DEEP-SEA RESEARCH
PART II

www.elsevier.com/locate/dsr2

Phycoerythrin-containing picocyanobacteria in the Arabian Sea in February 1995: diel patterns, spatial variability, and growth rates

Nelson D. Sherry[a,b,*], A. Michelle Wood[a]

[a]*Department of Biology, University of Oregon, Eugene, OR 97403, USA*
[b]*Department of Earth and Ocean Sciences, University of British Columbia, Vancouver, B.C. Canada, V6T 1Z4*

Received 15 December 1998; received in revised form 10 July 2000; accepted 11 August 2000

Abstract

The abundance of phycoerythrin-containing picocyanobacteria in the surface mixed layer was measured both along-shore and offshore between 8 and 23 February 1995 in the Northwestern Arabian Sea. Water samples from 3 m depth were taken at 2-h intervals and picocyanobacterial abundance and frequency of dividing cells were determined by epifluorescence microscopy. Cell counts showed an average diel change from a mid-day minimum of $\sim 50 \times 10^3$ cells ml^{-1} to an evening maximum of $\sim 180 \times 10^3$ cells ml^{-1}. The diel change was greater than the differences observed between physically and spatially discrete water masses. By counting the frequency of dividing cells (FDC) and using a novel approach to estimating the length of time required to complete cell division, growth and loss rates were both estimated to be $\sim 2.9\,d^{-1}$ with daily turnover being 140% of the mean standing stock. If differences in the intrinsic population growth rate (μ) and the net rate of change in cell number (r) are assumed to be due to grazing, then grazing occurred throughout the day at a relatively constant rate (reflecting phytoplankton loss rates of $\sim 0.12\,h^{-1}$). Cell division rates peaked in the late afternoon and early evening. FDC decreased throughout the night, suggesting that dark-inhibition of cell division is weak or nonexistent in the picocyanobacteria we studied. While all cell types included in this study would be identified as *Synechococcus* by flow cytometry because they were small unicells with bright phycoerythrin fluorescence, morphological variability suggests that the community was actually taxonomically diverse and included cells other than *Synechococcus*, including *Synechocystis*. Despite this diversity, the strong diel patterns we observed persisted throughout the study region, suggesting that great care should be taken when interpreting picocyanobacterial survey data and experimental results that do not account for the effects of time-of-day.

* Corresponding author. Present address: Department of Earth and Ocean Sciences, University of British Columbia, Vancouver, B.C. Canada, V6T 1Z4; Fax: +1-604-822-6091.
E-mail address: nsherry@interchange.ubc.ca (N.D. Sherry).

0967-0645/01/$ - see front matter
PII: S0967-0645(00)00138-7

1. Introduction

Phycoerythrin-containing picocyanobacteria have proven to be important primary producers in the Arabian Sea during all seasons of the year (Burkill et al., 1993; Veldhuis et al., 1997; Bidigare et al., 1997; Campbell et al., 1998; Garrison et al., 1998; Latasa and Bidigare, 1998; Barlow et al., 1999; Wood et al., 1999; Toon et al., 2000). This contrasts with early notions that picophytoplankton might dominate oligotrophic waters but be relatively unimportant in upwelling centers or nutrient-enhanced regions (Jochem et al., 1993; Veldhuis et al., 1997). Their notable presence in both oligotrophic and upwelling-influenced waters is, however, consistent with the capacity of marine *Synechococcus* to respond dramatically to increases in the nitrate concentration of oceanic waters (Glover et al., 1988), particularly at low latitudes (Lindell and Post, 1995; Morel, 1997). While the probability that larger phytoplankton will also grow well in nutrient-enriched waters means that *Synechococcus* and other phycoerythrin-containing picocyanobacteria may not dominate nutrient-enriched waters in the Arabian Sea, it is clear that upwelling-driven nutrient enrichment during the SW Monsoon leads to some of the highest concentrations of phycoerythrin-containing picocyanobacteria ever reported (Bidigare et al., 1997).

Survey of the general literature on *Synechococcus* in nature shows extensive evidence of diel patterns of growth and cell division (Waterbury et al., 1986; Campbell and Carpenter, 1986; Carpenter and Campbell, 1988; Pick and Bérubé, 1992; Vaulot et al., 1996). However, it is not known if grazing is continuous throughout a 24-h period or occurs primarily during the nighttime after cell division in prey populations has ceased. Resolution of this question is particularly important for the estimation of intrinsic growth rates for *Synechococcus* since, if grazing occurs continuously, many methods for determining growth rate will underestimate the true rate of intrinsic population growth because they do not account fully for losses due to grazing (Furnas, 1990). As noted by Waterbury et al. (1986), if grazing is continuous during periods of population growth, the net increase in cell number implies very high growth rates for many wild populations of *Synechococcus*.

In February 1995, we examined diel patterns of abundance and frequency of dividing cells (FDC) in phycoerythrin-containing cyanobacteria in surface waters of a large region of the northern Arabian Sea. While nearly all phycoerythrin-containing picocyanobacteria in our samples conformed to the general morphological description of marine *Synechococcus*, there was enough evidence for the presence of other types of cells (e.g., *Synechocystis* or other undescribed taxa) that we choose to use the term 'picocyanobacteria' to describe our target population rather than '*Synechococcus*'. However, it should be noted that the entire community of cells we studied would have been included in the cell types described as '*Synechococcus*' by investigators using flow cytometry to study picophytoplankton dynamics during the 1994–95 Arabian Sea expedition (e.g., Campbell et al., 1998; Liu et al., 1998; Brown et al., 1999; Tarran et al., 1999; Garrison et al., 2000). Our data set was obtained during a period of the 1994–95 seasonal cycle for which there are no other reports of picocyanobacterial abundance or growth rates, and provides needed insight into the dynamics of this community during the late NE Monsoon and Spring Intermonsoon. We also introduce a numerical technique to analyze the data that allows us to examine the question of whether or not grazing is continuous throughout the diel cycle.

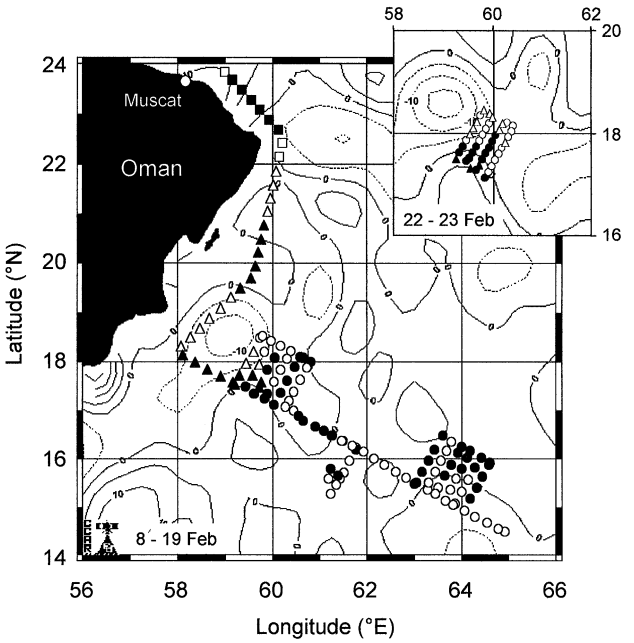

Fig. 1. Sampling locations for underway sampling during cruise TN044 of the R.V. *Thomas G. Thompson* are overlain on the TOPEX/ERS sea-surface height anomaly map for 12 February or (inset) 23 February (courtesy of Colorado Center for Astrodynamics Research). Filled symbols denote nighttime sampling locations and open symbols denote daytime sampling locations. Water mass types (Table 1, Fig. 3) are indicated by symbol shape: Gulf-influenced water (■), Coastal Water (▲), Offshore water (●); Inset: Resampling of western radiator, higher density water ($> 24.25\,\mathrm{kg\,m^{-3}}$; △) or lower density water ($< 24.22\,\mathrm{kg\,m^{-3}}$; ○).

2. Methods

2.1. Cruise track and sampling

Data presented here were collected during cruise TN044 (8–28 February 1995) aboard the R/V *Thomas G. Thompson* during the Spring Intermonsoon season of 1995 (Lee et al., 2000). For 12 days (8–14, 16–19, and 22–23 February) the ship sampled an established survey pattern using SeaSoar, a towed undulating profiling package; during the remainder of the cruise, discrete water samples were collected at hydrographic stations located along the survey track (Fig. 1; Lee et al., 2000). While the ship towed the SeaSoar, it traveled at a relatively constant speed of 8 knots. During that time, underway samples were withdrawn from the ship's flow-through seawater system for estimation of picocyanobacterial abundance, frequency of dividing cells (FDC), and fluorescence signature. Sampling intervals were every 2 h during the first pass of the survey pattern (8–19 February) and every hour during a resampling of the western radiator (22–23 February, Fig. 1). Other investigators sampled the flow-through system for underway measurement of pigments, nutrients, fluorescence properties, salinity, and temperature.

The intake for the ship's flow-through system was located at ~3 m, forward of the leading edge of the ship's keel; water flowed freely through the polypropylene-lined, steel-jacketed system, and took an estimated five minutes to flow from intake to the discharge point on the stern (George White, University of Washington, personal communication). Since the passage time was short and occurred in the dark, changes in picocyanobacterial cell abundance and FDC were assumed to be negligible in the flow-through system. Microscopic analysis of fresh material showed no evidence of cell lysis for picocyanobacteria or larger plankton cells. While some chains of large cells may have been broken into smaller chains, even large diatoms and dinoflagellates appeared intact. Nutrient data were collected underway using an autoanalyzer in line with the flow-through system; these data were comparable to those obtained from bottle samples and showed no evidence of nutrient elevation from cell lysis in the flow-through system (Burton Jones, University of Southern California, personal communication). Combined with our microscopic observations, this is relatively firm evidence that unbiased samples of picocyanobacteria could be collected from surface waters using the ship's flow-through system while the ship was underway.

2.2. Sample handling and processing

Underway samples were collected into 500 ml amber, polyethylene Nalgene bottles. Once collected, samples were usually processed immediately and were always stored in the cold (4°C) until filtered. From two time-series experiments lasting 25 h, it was determined that storage under these conditions did not detectably alter cell concentration, presumably because the temperatures were so much lower than ambient that metabolic activity in both grazers and picocyanobacteria was greatly inhibited. At each sampling time-point, samples for chlorophyll *a* were collected from the flow-through system, and values for temperature and salinity were recorded.

For enumeration of picocyanobacteria and determination of FDC, triplicate subsamples of 5–20 ml from each water sample were filtered at 10 kPa vacuum onto 25 mm, black, polycarbonate membrane filters with a 0.2 μm pore size (Nuclepore). The filters were then mounted on glass slides using immersion oil and counted by epifluorescence microscopy (Li and Wood, 1988). Of the three replicates, one was counted onboard (replicate C). All three replicate sets of slides were stored at −20°C during the cruise, packed in dry ice for shipping, and then stored at −80°C. Counting of the remaining replicate slides (A and B) was done between 19 May and 6 October 1995. No systematic differences in cell abundance were observed among the three replicates.

The phycoerythrin (PE) fluorescence signature was determined for each sample according to Wood et al. (1999). PE-containing picocyanobacteria may synthesize any of several spectral forms of PE; these differ in the relative abundance of phycoerythrobilin (PEB, λ_{AbsMax} ~550 nm) and phycourobilin (PUB, λ_{AbsMax} ~500 nm) chromophores. The relative abundance of PUB and PEB chromophores contributing to PE fluorescence was estimated by measuring the height of peaks near 500 and 550 nm in the fluorescence excitation spectra for PE emission at 564 nm and calculating a ratio ($500_{ex}/550_{ex}$). For each measurement, a single 50 ml subsample of each water sample was concentrated by filtration onto 0.2-μm Nuclepore filters. Following filtration, cells on the filters were resuspended in 4 ml cryovials with 3 ml of sample water. Excitation spectra (400–560 nm) for PE emission at 564 nm were analyzed using an Aminco-Bowman luminescence spectrometer with a 4 nm bandpass for both excitation and emission. Cell concentrates were stored in the cryovials at 4°C until analyzed, between 3 and 19 March 1995. As noted in Wood et al.

(1999), storage over this period of time does not appear to affect the shape of the fluorescence excitation spectra (and hence the $500_{ex}/550_{ex}$ ratio). Relative height of the fluorescence maxima at 500 and 550 nm were calculated for corrected spectra after subtracting blanks.

2.3. Cell counts and measurement

Cell counts were done at sea using a Zeiss Standard epifluorescence microscope at 1000× with a Zeiss 48-77-12 filter set (546 nm excitation, > 590 nm emission). Post-cruise cell counts were done on a Leitz Laborlux S epifluorescence microscope at 1000× with a Leitz M2 filter set (546 nm excitation, > 580 nm emission). Counting was done according to the following rules: as many grids (or fields of view) were counted as needed, up to a maximum of 30, to enumerate a minimum of 400 cells. A minimum of 4 grids, in different locations on the filters, were always counted even when fewer grids would have yielded counts > 400 cells. For one set of replicates, dividing cells in each grid were also counted. FDC was calculated as the ratio of dividing cells to the total cell abundance. Cells which had any visible sign of wall invagination, but which were not yet separated into two visibly distinct cells, were considered to be dividing.

Image analysis, using ImagePro Plus (Media Cybernetics, Silver Spring, MD), was used for determination of cell size in one set of replicates over two separate 24-h periods (12 and 18 February; western and eastern radiator locations, respectively). Color photographs were taken, under the same conditions as counting, with a PhotoAutomat attachment to the Leitz microscope. Two photographs were taken in different areas of each slide; fields were photographed if all visible cells were closely in focus. Each photograph was scanned with a Nikon CoolScan color film scanner to create 24-bit bitmapped images, 602 × 397 pixels, for processing with an effective pixel size of 0.17 × 0.17 μm.

Cell volume was calculated by geometric approximation using one of two equations depending on the size of the cell image. If the image area of the cell was ⩾ 10 pixels, the minimum for which the software was able to measure a maximum and minimum diameter, then the cell was assumed to be a rod with two hemispherical ends connected by a cylinder and the following equation was used:

$$V = \frac{4}{3}\pi\left(\frac{w}{2}\right)^3 + \pi\left(\frac{w}{2}\right)^2(l - w), \tag{1}$$

where V is volume in μm^3, w is minimum diameter (width) in μm, and l is maximum diameter (length) in μm. If the image area of the cell was < 10 pixels, then cell volume was calculated as a sphere according to

$$V = \frac{4}{3}\pi\left(\sqrt{\frac{A}{\pi}}\right)^3, \tag{2}$$

where A is area measured in μm^2.

For *Synechococcus* there are a number of published conversion factors ranging from 85 to 400 fg C μm^{-3}, with discussion of real values being even higher (Li, 1986). Recent studies in the Arabian Sea, including Campbell et al. (1998) and Liu et al. (1998), rely on a conversion factor of 175 fg C $cell^{-1}$. A back-calculation using the average cell volume from this study and 175 fg C $cell^{-1}$

gives a reasonable 230 fg C μm^{-3}. Thus 230 fg C μm^{-3} was used as the carbon to volume conversion in this study to allow direct comparisons to the other recent Arabian Sea literature on *Synechococcus*.

3. Results

3.1. Physical and climatological setting

Throughout the cruise, weather conditions were mild. Winds averaged 7 knots (range = 0.7–12) and glassy smooth sea surfaces were common. Within the context of the annual cycle of wind forcing and heat flux, this cruise began shortly after mid-basin heat flux reversed at the end of the Northeast Monsoon (Lee et al., 2000). Shipboard measurements showed weak surface cooling at the beginning of the cruise and then net surface warming during the final two weeks of the cruise (Lee et al., 2000).

Three general water types with slightly overlapping temperature and salinity characteristics were observed: (1) cool, high-salinity water from the Gulf of Oman was observed in the nine most northerly samples, (2) warmer, fresher coastal water was observed along the coast and half-way through the first western radiator, and (3) warm, salty offshore water was observed in the eastern half of the western radiator and all points further east (Table 1, Figs. 1–3). We refer to the water from the Gulf of Oman as "Gulf-influenced" water in both tables and Figs. 1, 3 and 4. Coastal water showed the greatest range in σ_T (Figs. 2 and 3). The cruise track crossed several fronts, notably the strong front between water from the Gulf of Oman and coastal water early in the cruise, fronts associated with a series of small-scale patches including a possible cold-core eddy, and the transition to high-salinity water between the western and eastern radiator (cf. Lee et al., 2000). Some of these features account for the variability in chlorophyll *a* concentration and other properties within the three major water mass types (Table 1). Offshore water east of the 'bowtie' and the eastern radiator had the highest combination of salinity and temperature (Table 1, Figs. 2 and 3).

Conditions in the western radiator changed slightly between the first sampling (11–13 February) and the resampling (22–23 February); most notable was the fresher water that had moved into the southeastern quadrat of the grid (Figs. 1 and 3; Sherry, 1995). This accompanied the intensification of an eddy that occupied the western part of the radiator (Fig. 1).

3.2. Biological observations

Microscopic analysis revealed the presence of small ($< 2\,\mu m$) unicellular PE-containing cells in all samples. The most common cell types were either short rods or cocci resembling marine *Synechococcus* as described by Waterbury et al. (1986) and Waterbury and Ripka (1989). In some samples, round cells between 1.25 and 2.0 μm in diameter, also were common; these were occasionally seen in packets of four or more cells. In other samples, rod-shaped cells also were seen in packets of four or more cells. At least some of these are probably *Synechocystis*, a genus of cyanobacteria distinguished from *Synechococcus* by the fact that cell division occurs in two planes rather than one (Waterbury and Ripka, 1989). Unless the cells were joined in tetrads, it was difficult

Table 1
Hydrographic characteristics of water sampled during this study. ND = no data collected

		Gulf-influenced	Coastal	Off-shore	W Radiator resampling[a]
Temperature (°C)					
	Maximum	24.7	25.3	26.2	25.5
	Minimum	24.4	24.7	24.9	24.6
	Average	24.5	24.9	25.3	25.0
	SD	0.1	0.2	0.3	0.2
	n	9	29	91	40
Salinity					
	Maximum	36.37	36.28	36.50	36.30
	Minimum	36.24	35.96	36.04	35.93
	Average	36.29	36.12	36.21	36.09
	SD	0.03	0.09	0.11	0.09
	n	9	29	91	40
Sigma-T ($kg\,m^{-3}$)					
	Maximum	24.53	24.40	24.28	24.40
	Minimum	24.40	24.04	24.05	23.96
	Average	24.47	24.22	24.15	24.18
	SD	0.04	0.10	0.04	0.12
	n	9	29	91	40
Abundance (10^3 cells ml^{-1})					
	Maximum	192	210	258	167
	Minimum	63	51	30	24
	Average	138	112	106	64
	SD	45	39	48	29
	n	9	29	92	40
	Time of Maximum	0000	2000–2200	1800–2200	0300–0500
	Time of Minimum	1600	0600–1600	1000–1400	0900–1700
Frequency of Dividing Cells					
	Maximum	0.95	0.86	0.87	0.55
	Minimum	0.04	0.03	0.03	0.04
	Average	0.45	0.25	0.28	0.27
	SD	0.43	0.22	0.21	0.14
	n	9	29	89	40
	Time of Maximum	1800	1040–1800	1030–1800	0600–1000
	Time of Minimum	0200	0400–0800	0400–0800	0000
$500_{ex}/550_{ex}$ Ratio					
	Maximum	0.96	1.40	1.85	ND
	Minimum	0.79	0.74	1.26	ND
	Average	0.87	1.18	1.53	ND
	SD	0.05	0.13	0.13	ND
	n	9	28	88	ND

Table 1 (*continued*)

	Gulf-influenced	Coastal	Off-shore	W Radiator resampling[a]
Chlorophyll (mg m^{-3})				
Maximum	1.33	1.65	2.31	1.25
Minimum	0.64	0.48	0.40	0.43
Average	0.93	0.77	0.97	0.81
SD	0.24	0.22	0.34	0.20
n	9	28	91	40

[a]Resurveyed 22–23 Feb in proximity to apparent cold–core eddy (Fig. 1); lower cell abundance is statistically significant ($p \ll 0.0001$).

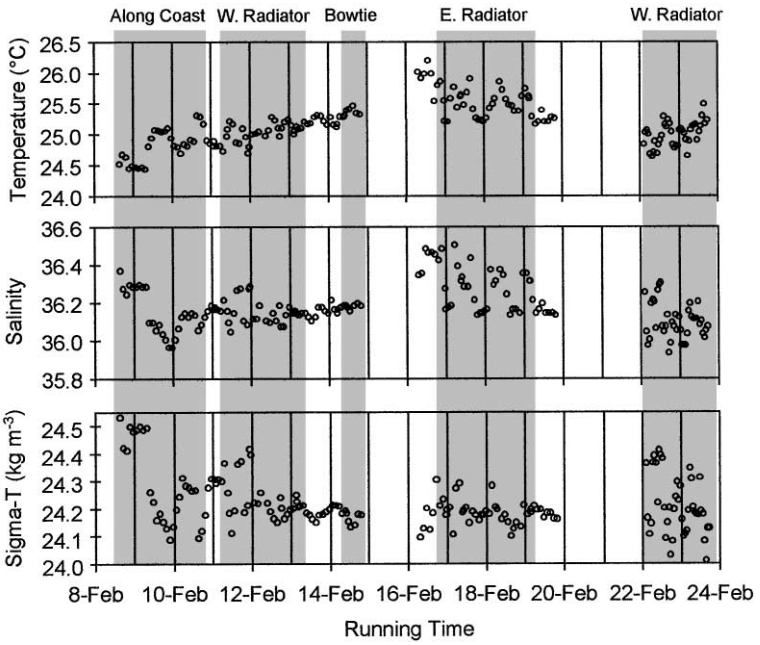

Fig. 2. Hydrographic data for all underway sampling points plotted according to sampling time. Shaded areas represent periods spent in specified regions along the cruise track.

to discriminate between these different cell types, so we treated the whole community of PE-containing picocyanobacteria as a single group in this study. This facilitates comparison of our results with essentially all other analyses of "*Synechococcus*" in the Arabian Sea because these other studies were based on flow cytometric analysis of PE-containing picocyanobacteria (e.g., Campbell et al., 1998; Liu et al., 1998; Brown et al., 1999; Tarran et al., 1999; Garrison et al., 2000). Flow cytometry uses the small size and characteristic PE fluorescence of marine *Synechococcus* to distinguish them from prochlorophytes and small eukaryotes; this procedure works well

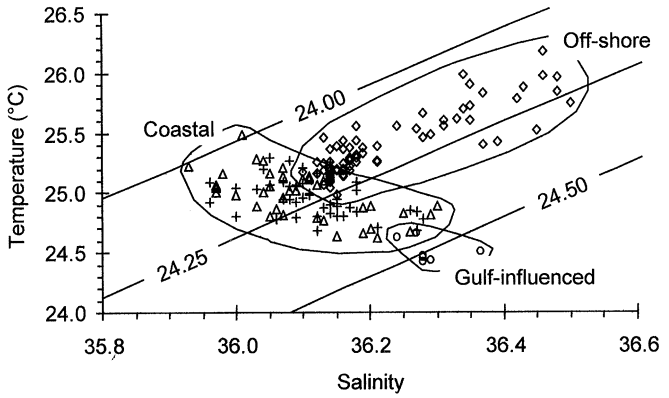

Fig. 3. T/S diagram of water at all underway sampling points grouped by water type. Data points indicate water from the Gulf of Oman (Gulf-influenced water) (○); coastal water, not including the second pass of the western radiator (△); water sampled during the second sampling of the western radiator (+); and offshore water (◇). Sloping lines represent lines of constant density (σ_T).

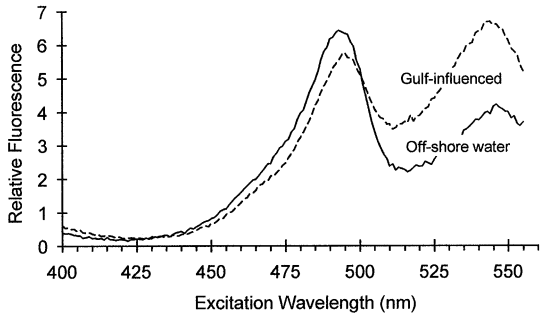

Fig. 4. Excitation spectra for phycoerythrin emission at 564 nm (± 2 nm) representative of typical samples from Gulf-influenced (- - -) and offshore water (—). Samples from 8 February 1200-h and 17 February 0400-h (local time), respectively.

when there are no other small phycoerythrin-containing taxa in the sample, but is not sufficient to distinguish *Synechococcus* from *Synechocystis*. Using the strictly optical criteria usually used to identify *Synechococcus* in natural samples by flow cytometry, all cells we counted would be identified as "*Synechococcus*".

The PE fluorescence excitation spectra always showed two well-defined peaks, one at wavelengths absorbed by PUB and one at wavelengths absorbed by PEB. In no instance did we find evidence that cells synthesizing PUB-lacking PEs dominated the picocyanobacterial community (Fig. 4). In Gulf-influenced water, the $500_{ex}/550_{ex}$ fluorescence ratio was always < 1.0. Except for three samples farther south along the coast, this was the only water showing a $500_{ex}/550_{ex}$ fluorescence ratio < 1.0 (Table 1, Fig. 5). Coastal water showed the greatest range in the $500_{ex}/550_{ex}$ fluorescence ratio (Table 1, Fig. 5), and offshore water was nearly always characterized by communities with a high $500_{ex}/550_{ex}$ fluorescence ratio (Table 1, Figs. 4 and 5).

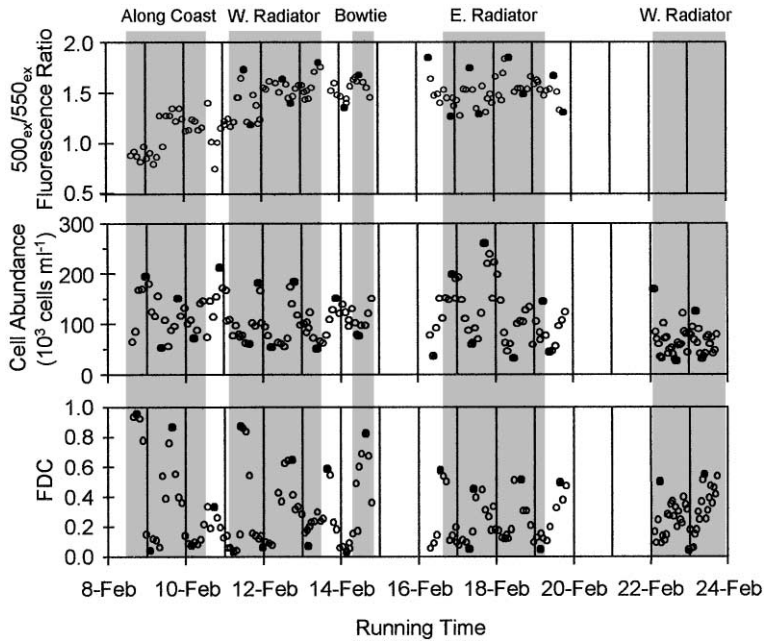

Fig. 5. Biological properties for all underway sampling points plotted according to sampling time. Shaded areas represent periods spent in specified regions along the cruise track. Filled data points were used as daily minimum and maximum values in calculating rates of change during daily periods of increase and decrease in cell abundance (Table 2).

Cell concentration ranged from 30,000 to 258,000 cells ml^{-1}, with both the highest abundance and greatest range in abundance observed in offshore water (Table 1, Fig. 5). However, these summary statistics are greatly misleading since average concentrations were around 100,000 cells ml^{-1} in all areas (Table 1, Fig. 5). The most striking feature of cell abundance data is the strong diel trend. During essentially every 24-h sampling period, cell abundance regularly increased from a mid-day minimum of around 50,000 cells ml^{-1} to a nighttime maximum of around 180,000 cells ml^{-1} (Fig. 5). Over a given 24-h period, there was little net change in cell abundance, despite the fact that there were periods of rapid population increase every day (Fig. 5). FDC also showed a strong diel trend, reaching a minimum between 3 and 11.5% after midnight and before dawn (Fig. 5). Cell size, while only reported for two of the 24-h sampling periods, showed peaks in cell volume and length:width ratio at about the same time as the peak in FDC (Fig. 6).

We explored the effects of time-of-day, sampling location, and water mass type on cell abundance and FDC using two-way analysis of variance. With sampling location divided into three groups (Gulf-influenced, coastal, offshore) based on the water mass properties in Table 1, we found that location did not have a significant effect on either cell abundance or FDC. If we split the data into four groups by separating the second re-sampling of the western radiator into a fourth category, location had a significant effect on cell abundance (but not FDC) that was independent of the effects of time of day. This appeared to be due to the relatively lower cell abundance observed during the second resampling of the western radiator when compared to abundance observed in all

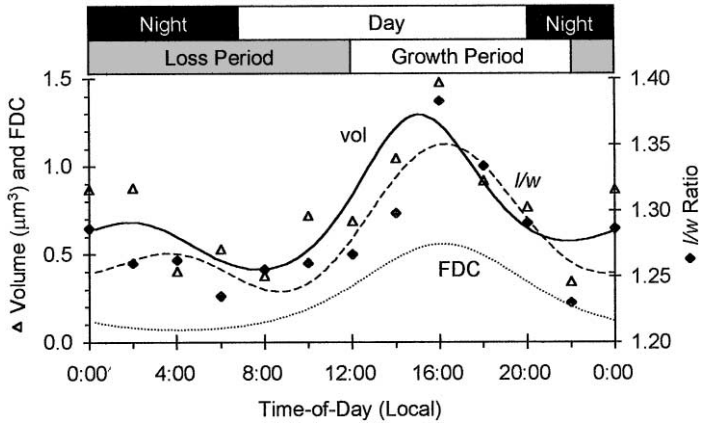

Fig. 6. Cell volume (△, —) and l/w (◆, - - -) ratio relative to time-of-day and frequency of dividing cells, FDC (⋯). Data points are averages of the values from 12 and 17 Feb. GMT ($n = 2$). Trend lines are the least-squares, best fit, 2 term Fourier series.

other areas ($p < 0.0001$ by Student's t-test). In both analyses, time of day had a highly significant effect on FDC, but if the effects of time of day are accounted for, location and water mass type did not have a significant effect on FDC.

Samples collected successively in time showed consistent trends, with cell abundance either increasing or decreasing depending on the time of day (Fig. 5). We examined day-to-day variation in the apparent rates of increase or decrease by calculating rates of change in cell number during each period of loss and gain assuming an exponential model for population growth (Table 2). While location and time were confounding variables with this type of analysis, the close spacing of the samples meant that, in general, the same water mass was being sampled during each 24-h period (Table 2). This analysis showed that, for any given 24-h period, loss rates during the period of decrease were roughly comparable to gain rates during the period of increase. The possible exception to this pattern occurred during the second resampling of the western radiator when loss rates may have been greater than gain rates (Table 2). Average rates of change were about $0.10\,h^{-1}$ in the Gulf-influenced water, coastal water, and offshore water sampled 9–13 February, and higher (0.13–$0.16\,h^{-1}$) in the offshore water of the eastern radiator sampled 16–19 February. Average rates of increase and decrease, calculated for all eleven periods of increase and decrease indicate that loss rates balanced gain rates in the region overall (Table 2).

4. Discussion

These data showed a consistent pattern in which remarkable increases in cell abundance were essentially balanced by equally remarkable decreases in cell numbers every day across a wide geographic area. Net population growth over a daily cycle was very low, but intrinsic growth rates appeared to be high. For example, the hourly rates of increase of $0.11\,h^{-1}$ observed during the first six sampling days would translate to population growth of $\sim 1.32\,d^{-1}$ if growth occurred over the

Table 2
Rates of cell increase and decrease calculated from the maximum and minimum cell abundances each day[a]

Local time	Δtime (h)	Abundance (10^3 cells ml^{-1})	Increase/decrease Rate (h^{-1})	Hydrographic location[b]
02/09/95 00:00		192		
02/09/95 10:00	10.0	51	− 0.13	Gulf-influenced & Coastal
02/09/95 20:00	10.0	149	0.11	Coastal
02/10/95 06:00	10.0	70	− 0.08	Coastal
02/10/95 22:00	16.0	210	0.07	Coastal
02/11/95 16:00	18.0	59	− 0.07	Coastal
02/11/95 22:00	6.0	179	0.19	Coastal & off-shore
02/12/95 06:00	8.0	52	− 0.15	Coastal & off-shore
02/12/95 20:15	14.3	181	0.09	Coastal & off-shore
02/13/95 10:00	13.8	49	− 0.09	Off-shore
02/13/95 22:00	12.0	149	0.09	Off-shore
02/14/95 12:00	14.0	75	− 0.05	Off-shore
02/16/95 10:00		34		
02/16/95 22:00	12.0	197	0.15	Off-shore
02/17/95 10:00	12.0	57	− 0.10	Off-shore
02/17/95 18:00	8.0	258	0.19	Off-shore
02/18/95 12:00	18.0	30	− 0.12	Off-shore
02/19/95 06:00	18.0	143	0.09	Off-shore
02/19/95 10:00	4.0	42	− 0.31	Off-shore
02/22/95 03:00		167		
02/22/95 17:00	14.0	24	− 0.14	W. Radiator Resampling
02/23/95 05:00	12.0	123	0.14	W. Radiator Resampling
02/23/95 09:00	4.0	29	− 0.36	W. Radiator Resampling
Average maximum		177 (SE = 12)		
Average minimum		48 (SE = 5)		
Average rate of increase			0.12 (SE = 0.02)	
Average rate of decrease			− 0.15 (SE = 0.04)	

[a]Rates were calculated as the difference between the natural log of each consecutive minima and maxima divided by elapsed time (ΔTime).
[b]Physical and biological properties given in Table 1.

12-h light period and there was no grazing during the period of cell increase. Loss rates of 0.10 h^{-1}, as calculated for the periods of cell loss during the same six days, could only be balanced by population growth rates on the order of 2.4 d^{-1}, if grazing was maintained at that rate over a 24-h cycle. Such growth rates are not outside the realm of possibility for picocyanobacteria (cf. Waterbury et al., 1986; Kudoh et al., 1990), but do exceed most reports from the Arabian Sea. One condition that might reconcile our observations with estimated growth rates of ~ 1 d^{-1} (cf. Burkill et al., 1993; Brown et al., 1999) is that of discontinuous grazing. In nearly all cases, the loss rates we measured during periods of decrease were comparable to gain rates during periods of increase.

Furthermore, the diel pattern of FDC indicates that cell division is definitely discontinuous and phased to occur in the late afternoon. Herbivores could utilize a variety of environmental cues to time grazing activity so that it occurred during periods of highest prey density after cell division was complete. If this occurred, and cell division occurred only during periods we define as periods of increase and grazing only occurred during periods we define as periods of population decrease, then picocyanobacterial growth rates would range between 1.0 and $1.5\,d^{-1}$.

The growth rates we calculated for periods of decrease and increase represent estimates of net population growth. Net population growth rates (r) are typically described as the difference between intrinsic growth rates (μ) and loss or mortality rates. Differences between r and μ reflect grazing rates if we assume that all other sources of cell loss are minimal. In order to explore our data for further evidence of high growth rates in the picocyanobacterial community, we have used our data on FDC to estimate μ by a modification of the FDC technique described by McDuff and Chisholm (1982). One of the difficulties with this approach to measuring growth rate is the need for an estimate of the time cells spend in cytokinesis (t_d). We have approached this problem by pooling the data from our repeated 24-h sampling periods to obtain single, best-fit, curves representing the average diel trend in cell abundances and FDC (Fig. 7a). A single curve representing the average diel pattern for net population growth (r) was calculated from the rate of change in cell abundance; t_d was then derived from the length of the temporal offset of the peak in r and FDC (7b; see below). Fig. 7a can be viewed as a summary figure for the data presented in Fig. 5; we chose to include all data from the cruise to maximize the degree to which region-to-region variability was incorporated into our overall view of the region. While other investigators might choose to pool different subsets of the data, we believe this approach provides the best summary and is justified based on the consistency of the timing and magnitude of daily maxima and minima in both cell abundance and FDC, the results of the analysis of variance, the relative constancy of daily means in cell abundance, and the obvious persistence of the diel pattern observed in Fig. 5.

Our purpose in summarizing the data this way was to examine the data for general evidence that basin-wide growth rates of picocyanobacteria were either on the order of $1\,d^{-1}$, or considerably higher. By obtaining a good estimate of μ that could be compared to an estimate of r calculated from the same pooled data, we also were able to test the hypothesis that grazing is discontinuous over the diel cycle. We predicted that, if grazing occurs only during the night after prey concentrations are maximal, there would be a diel cycle in the difference between μ and r with a daily maximum during the period of highest grazing rates. If grazing occurred throughout the day, then we predicted that the difference between μ and r would be relatively constant throughout the day and the hypothesis of discontinuous grazing would have to be rejected.

4.1. Estimation of μ and r from pooled data

Data collected from each of the 12 sampling points in a 24-h day (2-h spacing) were averaged together for harmonic analysis (Fig. 7a). Using the best-fit diel trend lines, net population growth (r) was estimated from changes in cell abundance and the intrinsic population growth rate (μ) was estimated from FDC. The rate of change (r) of abundance (N) was calculated for each of the 12 sampling times ($t = 0, 2, 4, \ldots, 22$) throughout the diel cycle. Rate calculations were based on the observed change in average cell abundance between the time points before ($t - 2$) and after ($t + 2$)

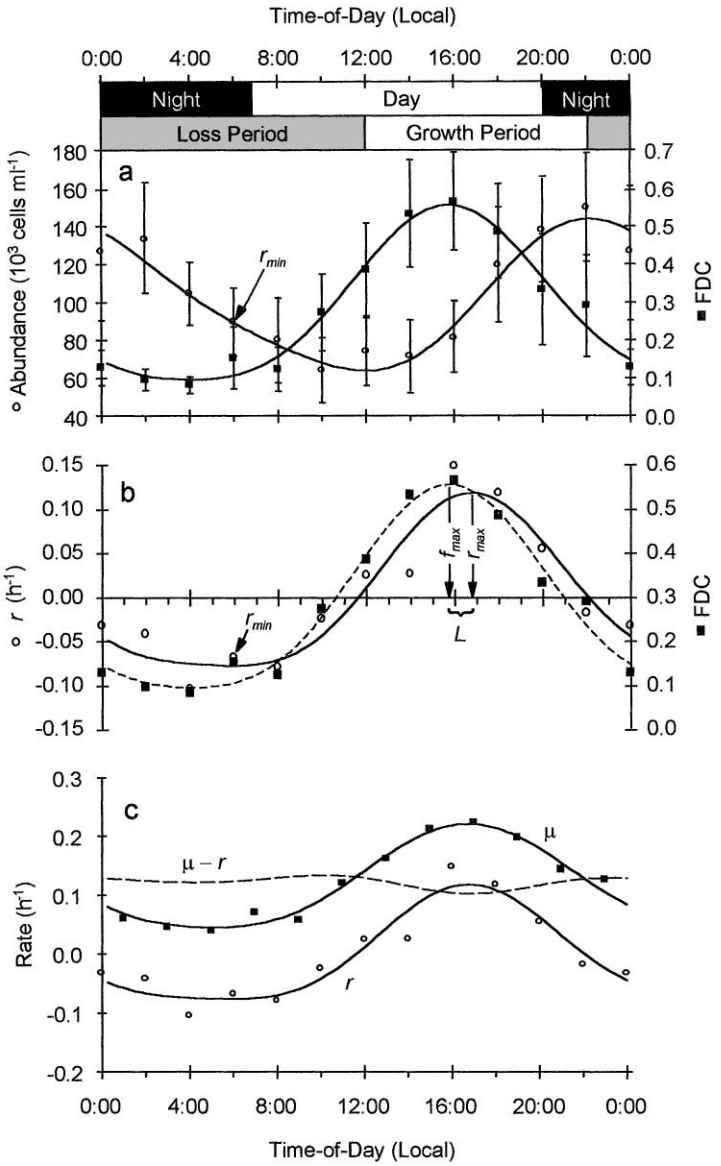

Fig. 7. (a) Cell abundance (○) and frequency of dividing cells, FDC (■) relative to time-of-day. Data points represent means for all days sampled ($n \geqslant 8$). Error bars indicate $\pm$ 2 SE. Trend lines are the least-squares, best fit, 2 term Fourier series giving $R^2 = 0.41$ for abundance and $R^2 = 0.68$ for FDC. (b) Determination of lag time (L) between the peak in frequency of dividing cells, FDC (■, - - -) and the peak in population rate-of-change, r (○, —). Data points represent means for all underway sampling points ($n \geqslant 8$). Trend line is the sum-of-squares, best fit, 2 term Fourier series. (c) Calculation of grazing rate, μ–r (- - -), from the difference between the population rate of change r (○), and the division rate μ (■). Trend lines are the least-squares, best fit, 2 term Fourier series.

any given time point (t). Given

$$N_t = N_0 e^{rt}, \tag{3}$$

then

$$r = \frac{\ln(N_t/N_0)}{t} \tag{4}$$

and specifically

$$r_t = \frac{\ln(N_{t+2}/N_{t-2})}{\Delta t}, \tag{5}$$

where $\Delta t = 4$-h.

Just as in the raw data (Fig. 5), the diel fluctuations in cell abundance showed distinct periods, one during which there was a net addition of cells to the population and one during which there was a net loss of cells (Fig. 7a). Despite the large geographic area covered by this survey, and the fact that samples were collected from several water mass types dominated by at least two different spectral forms of picocyanobacteria, the variance in cell abundance and FDC measured at any given time of day was remarkably low (note that error bars in Fig. 6a reflect $2 \times$ SE).

FDC analysis provides an estimate of the intrinsic rate of growth of a population, independent of grazing rates. FDC analysis requires knowledge of the length of time during which the cells were in observable cytokinesis (t_d). We calculated t_d empirically from the lag time (L) observed between the peak in cell division (f_{max}) and the corresponding peak (r_{max}) observed in the rate of change of the cell abundance (r) (Fig. 4b).

L was estimated from the following equation:

$$L = t_{r\,max} - t_{f\,max}, \tag{6}$$

where $t_{r\,max}$ is the time of the peak in r and $t_{f\,max}$ is the time of the peak in FDC (Fig. 7b).

Since t_d is defined as the time during which visible cytokinesis is taking place, then on average, dividing cells counted at time t would have completed division and contributed to an increase in cell abundance at time $t + t_d/2 (= t + L)$ and therefore, $t_d = 2L$. A t_d of 2-h was determined based on the 1-h lag time between the peaks in FDC and r (Fig. 7b).

Using the derived t_d, instantaneous growth rates (μ), independent of grazing, were determined for each of the 12 diel time points by modifying the FDC equation presented by McDuff and Chisholm (1982) as follows:

From

$$\mu = \frac{1}{nt_d} \sum_{i=1}^{n} \ln(1 + f_i) \tag{7}$$

to

$$\mu_{(t+t_d/2)} = \frac{\ln(1 + f_i)}{t_d}, \tag{8}$$

where n is the number of evenly spaced sampling intervals per unit time and f_i is the observed FDC during the ith sampling period. Eq. (7) gives a growth rate (μ) averaged over n sampling

periods. To calculate μ for a specific sampling time, the lag time (L) had to be accounted for, because cells counted as dividing do not contribute to the population until a later time. So, μ calculated from FDC at time t was actually the division rate at $t + (t_d/2)$. Based on FDC, the intrinsic growth rate for the picocyanobacterial population was calculated to be $\sim 2.9\,d^{-1}$, with a 3.2-h doubling time during peak division.

To address the hypothesis that grazing was discontinuous during the day, the actual diel loss patterns were determined by subtracting the rate of change of the cell abundance (r) from the intrinsic growth rate (μ) for each of the 12 time-of-day points and fitting a curve to each of the 12 data points (Fig. 7c). The nearly constant difference between r and μ is consistent with the hypothesis that grazing was continuous over the diel cycle and that a relatively constant proportion of the population was lost at any given time.

4.2. Biomass and turnover rates

From the data in Fig. 6, the average cell volume was calculated to be 0.76 (SE = 0.09) μm^3 providing 175 (SE = 30) fg C cell^{-1} based on 230 fg C μm^{-3} (Fig. 5). The average of 101×10^3 cells ml^{-1} thus represented an average POC contribution by picocyanobacteria of 17×10^{-3} g C m^{-3}. Using the time-of-day curves fit to μ and N, the growth rate times the cell concentration was calculated for every 15 minutes and integrated over 24-h. This predicted an input of 140×10^3 cells ml^{-1} d^{-1} representing a carbon turnover rate of 24×10^{-3} g C m^{-3} d^{-1} or $\sim 140\%$ of the mean biomass and $> 290\%$ of the average daily minimum.

4.3. Implications and caveats

The merits and weaknesses of FDC growth rate analysis have been discussed extensively in the literature (McDuff and Chisholm, 1982; Campbell and Carpenter, 1986; Affronti and Marshall, 1994; Binder and Chisholm, 1995). The basic theory behind the FDC model is sound if certain assumptions are accepted. The assumptions, as stated by Campbell and Carpenter (1986, p. 140), are "(1) the duration of [identifiable] division (t_d) is constant with respect to changing environmental conditions, (2) t_d is identical for all cells in a population, and (3) all cells in a population are active". Beyond these assumptions, two further points should be considered when dealing with a wild population: (1) the level of preferential grazing on dividing cells must not be significant, and (2) a reasonable average t_d must be determined for the wild population being studied since t_d is unlikely to be identical for all cells in the population.

These assumptions can be addressed in various ways for our data. Preferential grazing on dividing cells could result in an overestimate of the actual growth rate since dividing (typically larger) cells might be preferentially removed by grazing between the time they were counted and the time when division was completed. If the rate of preferential grazing (G_p), is defined as the difference between the grazing rate on dividing cells and the average grazing rate on the population as a whole, and G_p can be estimated, then the following modifications to Eq. (7) would provide a μ corrected for preferential grazing:

$$\mu = \frac{1}{nt_d} \sum_{i=1}^{n} \ln(1 + f_i e^{-G_p(t_d/2)}). \tag{9}$$

If grazing is not constant over all n observations, then G_p is variable and must be calculated separately for each interval i.

We estimated the potential effects of preferential grazing in this study with an approximation of G_p derived from the force-balance model of Monger and Landry (1990, 1991) and by entering that value into Eq. (9). Assuming that, on average, dividing cells have 50% more volume than non-dividing cells, then the radius of a spherical cell is increased by 14% and the force-balance model provides the following:

$$\mathrm{PCCR} = \left(\frac{R_{\mathrm{div}}}{R_{\mathrm{avg}}}\right)^{0.9} = \left(\frac{1.14}{1}\right)^{0.9} = 1.13, \tag{10}$$

where PCCR is the predicted clearance rate ratio, R_{div} is the radius of the average dividing cell, and R_{avg} is the radius of the average cell in the population. Then G_p is calculated as $(\mathrm{PCCR} \times G) - G$ or $(1.13 \times 0.12) - 0.12 = 0.016$. Using a G_p of 0.016 in Eq. (9), we calculate μ to be $\sim 1.5\%$ lower than was otherwise calculated without accounting for preferential grazing. Therefore, the error introduced by preferential grazing was inconsequential.

Binder and Chisholm (1995) address these assumptions in relation to cell cycles in marine *Synechococcus* and suggest that t_d is constant for "fast-growth" cells that exhibit a generation time such that multiple chromosomal replication events must occur simultaneously. However, for slower growing cells, which divide between each chromosomal replication event, t_d can vary with growth rate. Liu et al. (1998) found > 2 copies of the genome in upper water column *Synechococcus* in the Arabian Sea. The patterns presented in this study show multiple rapid divisions at the end of the day with little cell growth occurring between the divisions, which further suggests the likely presence of multiple genomes. Binder and Chisholm (1995) note that blocked cell division, so long as it is not blocked during cytokinesis, does not affect the evaluation of t_d. Given evidence that some, but not all, strains of *Synechococcus* cannot complete cell division in the dark (Armbrust et al., 1989; Binder and Chisholm, 1995), we have to recognize that our growth rate estimates based on FDC could be high. However, the steady and dramatic decrease in FDC throughout the night suggests that dark-inhibition of cytokinesis was incomplete or absent in the populations we studied (Binder and Chisholm, 1995).

From appearance under the microscope and $500_{\mathrm{Ex}}/550_{\mathrm{Ex}}$ ratios, it was evident that there was more than a single cell type present in this picocyanobacterial assemblage. Data from three other SeaSoar cruises also show that the PE-containing picocyanobacterial community in the Arabian Sea is composed of a variety of morphological cell types during other seasons (A.M. Wood, unpublished data, cf. Lee et al., 2000, for cruise dates). It is probable that nearly all studies of '*Synechococcus*' in the Arabian Sea that are based on flow cytometry actually pool data from populations of different clones of *Synechococcus, Synechocystis* and, possibly, other undescribed picocyanobacteria (cf. discussion in Campbell et al., 1998). It is unlikely that all the different cell types shared the same t_d. However, if we accept the evidence that grazing occurred at a constant rate throughout the day, the maximum rate of cell loss observed in the pooled data ($\sim 0.113\,\mathrm{h}^{-1}$, Fig. 7b) can be used to estimate the grazing rate during the complete diel cycle. If this loss is balanced by growth, then the growth rate must be $\sim 2.7\,\mathrm{d}^{-1}$ (Sherry, 1995). This is an estimate of picocyanobacterial growth rates obtained from the pooled data that does not require an estimate of t_d. The degree of consistency between this estimate and the estimate made from FDC ($\sim 2.9\,\mathrm{d}^{-1}$) is

a further indication that our estimate of t_d was reasonable and that average picocyanobacterial growth rates in this region greatly exceeded $1\,d^{-1}$ during the Spring Intermonsoon. Of greater interest than variability introduced by differences in t_d among cell types is the degree to which this community showed persistent patterns across a wide geographic region. The growing evidence that cyanobacterial cell cycles are regulated by a circadian clock (Sweeney and Borgese, 1989; Golden et al., 1997; Shalapyonok et al., 1998; Johnson and Golden, 1999) may explain why diel patterns of FDC were relatively consistent.

The range of cell concentrations reported for surface waters in the Arabian Sea during four different seasons in 1994–95 (Campbell et al., 1998) corresponds with the range of cell concentrations we found over a single diel cycle in most of the areas we sampled. This brings assumptions about spatial variability into sharp question and indicates that survey data need to be corrected for time of day effects. With the exception of Liu et al. (1998), who reported *Synechococcus* growth rates $> 2\,d^{-1}$ at mesotrophic onshore stations during both the NE and SW Monsoon seasons, we have found no other reports of picocyanobacterial growth or loss rates in the Arabian Sea that are close to those calculated from our data.

While diel patterns might, at first glance, be explained away by postulating changes in either grazing rates or a combination of changes in grazing and growth rates, FDC is a grazing-rate independent calculation. When growth rates calculated by this method are compared to the rate of change in cell concentration, grazing rates appear to be constant throughout the day (Fig. 7c). Diel patterns in cell concentration of the type and magnitude observed in this study also might be explained by vertical mixing if cells were killed near the surface during the day and replenished from below with deeper mixing at night. However, with the exception of the southern coastal region of the cruise track, there was no evidence for a strong subsurface chlorophyll *a* or particle peak (Lee et al., 2000) and growth rates calculated from FDC accounted for both the timing and magnitude of the diel concentration pattern.

5. Conclusions

The data show a persistent diel trend in cell abundance of picocyanobacteria in the Arabian Sea during the early Spring Intermonsoon season. Picocyanobacterial abundance varied from roughly 50,000 to 180,000 cells ml^{-1} on a diel cycle that appeared to originate with phased cell division that occurred in the late afternoon and early part of the night. Our data on cell volume showed a maximum that appeared to coincide with the peak in FDC. Cell volume during the period of peak cell division was 3–6 times greater than it was during times of minimum division rate (Fig. 6). This implies that a series of rapid divisions took place with little cell growth occurring between them. The presence of multiple copies of DNA, as suggested by Liu et al. (1998) for *Synechococcus* in this region, also would suggest this type of division cycle.

From the timing of the diel pattern, several interesting physiological and ecological speculations can be made. Since division occurs in the afternoon and evening, there may be a daily quantum flux threshold which stimulates the beginning of the division process. Variation in mRNA content of coastal *Synechococcus* communities was dependent on cell division phased to the irradiance cycle (Kramer and Singleton, 1993), and diel patterns of ribulose bisphosphate carboxylase gene expression in picocyanobacteria appear to be tied to light cues (Pichard et al., 1996, but cf. Wyman,

1999). When expressed, these patterns conform to the model of a quantum flux threshold for some cell processes. Additionally, there may be an irradiance-based disadvantage to dividing during periods of highest photon flux such as reduced photosynthetic efficiency or increased DNA replication error or other cell damage due to high light during the division process.

We calculate growth rates of $\sim 2.9\,d^{-1}$, balanced by cell losses that are presumed to result from grazing. Because they were calculated from data obtained by analyzing unmanipulated water samples collected directly from nature, it is unlikely that they are biased by experimental artifact. Though the growth rates reported here are high, they are not unreasonable; Waterbury et al. (1986) reports daily growth patterns for *Synechococcus* that suggest that μ may be as high as $4.5\,d^{-1}$ (3.7-h doubling time) in the Sargasso Sea. Kudoh et al. (1990) found cyanobacterial growth rates in the north Pacific Ocean of $2.4\,d^{-1}$ (7-h doubling time), and Liu et al. (1998) report maximal growth rates $> 2\,d^{-1}$ in the Arabian Sea compared to the $2.9\,d^{-1}$ (6-h doubling time) reported here. Veldhuis et al. (1997) also observed relatively high growth rates ($1.3–1.9\,d^{-1}$) for *Synechococcus* in the Somali Basin during the 1993 Northeast Monsoon.

Our data indicate that grazing activity was continuous throughout the day and suggest a tight interdependent relationship between grazing and growth where daily turnover of picocyanobacteria was $\sim 140\%$ of the average standing stock. This pattern persisted over a large area in both coastal and offshore waters. It encompassed different picocyanobacterial communities over several days implying a near-equilibrium community dynamic. Close coupling of picocyanobacteria and protozoan grazing activity in the Arabian Sea was first suggested by Burkill et al. (1993). Balanced growth and loss rates also were observed for *Synechococcus* during the 1992–93 Northeast Monsoon (Reckermann and Veldhuis, 1997) and appear to be a general feature of this region (Landry et al., 1998; Brown et al., 1999; Caron and Dennett, 1999).

The diel patterns we observed pose a problem for investigators who do not account for them. Cell counts, physiological rate measurements, and short-term incubation experiments, unless specifically designed to account for diel effects, could be biased by the time of day at which they were conducted, while studies suggesting patchiness or other patterns in space may actually reflect nothing more than variability in the time of day during which sampling was done.

Acknowledgements

We thank Richard Castenholz, Russell Lande, and Sharon Smith for their support and suggestions in the development and completion of this manuscript. We also thank Ken Brink, Craig Lee, Burt Jones and the WHOI SeaSoar team and Zahit Uysal, Harib Al-Habsi and Rashid Al-Shihi for shipboard assistance and advice, Dave and Doug Phinney for their help in collecting samples and allowing us to use their chlorophyll *a* data, Craig Everroad and Zahit Uysal for their dedication to counting slides, Michael Lipsen for processing of the fluorescence data and the crew of the R/*V Thomas G. Thompson* for all their help. This research was supported by ONR grants N0014-94-1-0429 and N00014-99-1-0177 (to AMW) and N00014-94-1-0298 (to C.S. Yentsch and D. Phinney) and through an NRL/ASEE summer faculty fellowship to AMW under ONR program element 61135 of the ONR/NRL 6.1 ARI "Forced Upper Ocean Dynamics". This is US JGOFS contribution number 529.

References

Affronti L.F. Jr., Marshall, H.G., 1994. Using frequency of dividing cells in estimating autotrophic picoplankton growth and productivity in the Chesapeake Bay. Hydrobiologia 284, 193–203.

Armbrust, E.V., Bowen, J.D., Olson, R.J., Chisholm, S.W., 1989. Effect of light on the cell cycle of a marine *Synechococcus* strain. Applied and Environmental Microbiology 55, 425–432.

Barlow, R.G., Mantoura, R.F.C., Cummings, D.G., 1999. Monsoonal influence on the distribution of phytoplankton pigments in the Arabian Sea. Deep-Sea Research II 46, 677–699.

Bidigare, R.R., Latasa, M., Johnson, Z., Barber, R.T., Trees, C.C., Balch, W.M., 1997. Observations of a *Synechococcus*-dominated cyclonic eddy in open-oceanic waters of the Arabian Sea. Proceedings of the Society of Photo-optical Instrumentation Engineers 2963, 260–265.

Binder, B.J., Chisholm, S.W., 1995. Cell cycle regulation in marine *Synechococcus* sp. strains. Applied and Environmental Microbiology 61, 708–717.

Brown, S.L., Landry, M.R., Barber, R.T., Campbell, L., Garrison, D.L., Gowing, M.M., 1999. Picophytoplankton dynamics and production in the Arabian Sea during the 1995 southwest monsoon. Deep-Sea Research II 46, 1745–1768.

Burkill, P.H., Leakey, R.J.G., Owens, N.J.P., Mantoura, R.F.C., 1993. *Synechococcus* and its importance to the microbial foodweb of the northwestern Indian Ocean. Deep-Sea Research II 40, 773–782.

Campbell, L., Carpenter, E.J., 1986. Diel patterns of cell division in marine *Synechococcus* spp. (Cyanobacteria): use of the frequency of dividing cells technique to measure growth rate. Marine Ecology Progress Series 32, 139–148.

Campbell, L., Landry, M.R., Constantinou, J., Nolla, H.A., Brown, S.L., Liu, H., Caron, D.A., 1998. Response of microbial community structure to environmental forcing in the Arabian Sea. Deep-Sea Research II 45, 2301–2325.

Caron, D.A., Dennett, M.R., 1999. Phytoplankton growth and mortality during the 1995 Northeast Monsoon and Spring Intermonsoon in the Arabian Sea. Deep-Sea Research II 46, 1665–1690.

Carpenter, E.J., Campbell, L., 1988. Diel patterns of cell division and growth rates of *Synechococcus* spp. in Long Island Sound. Marine Ecology Progress Series 47, 179–183.

Furnas, M.J., 1990. In-situ growth rates of marine phytoplankton: approaches to measurement, community and species growth rates. Journal of Plankton Research 12, 1117–1151.

Garrison, D.L., Gowing, M.M., Hughes, M.P., 1998. Nano- and microplankton in the northern Arabian Sea during the Southwest Monsoon, August–September 1995 A US-JGOFS study. Deep-Sea Research II 45, 2269–2299.

Garrison, D.L., Gowing, M.M., Hughes, M.P., Campbell, L., Caron, D.A., Dennett, M.R., Shalapyonok, A., Olson, R.J., Landry, M.R., Brown, S.L., Liu, H., Azam, F., Steward, G.F., Ducklow, H.W., Smith, D.C., 2000. Microbial food web structure in the Arabian Sea: a US JGOFS study. Deep-Sea Research II 47, 1387–1422.

Glover, H.E., Prezelin, B.B., Campbell, L., Wyman, M., 1988. A nitrate-dependent *Synechococcus* bloom in surface Sargasso Sea water. Nature 331, 161–163.

Golden, S.S., Ishiura, M., Johnson, C.H., Kondo, T., 1997. Cyanobacterial circadian rhythms. annual review of plant physiology and plant molecular biology 48, 327–354.

Jochem, F.J., Pollehne, F., Zeitzschel, B., 1993. Productivity regime and phytoplankton size structure in the Arabian Sea. Deep-Sea Research II 40, 711–735.

Johnson, C.H., Golden, S.S., 1999. Circadian programs in cyanobacteria: adaptiveness and mechanism. Annual Review of Microbiology 53, 389–409.

Kramer, J.G., Singleton, F.L., 1993. Measurement of rRNA variations in natural communities of microorganisms on the Southeastern U.S. continental shelf. Applied and Environmental Microbiology 59, 2430–2436.

Kudoh, S., Kanda, J., Takahashi, M., 1990. Specific growth rates and grazing mortality of chroococcoid cyanobacteria *Synechococcus* spp. in pelagic surface waters in the sea. Journal of Experimental Marine Biology and Ecology 142, 201–212.

Landry, M.R., Brown, S.L., Campbell, L., Constantinou, J., Liu, H., 1998. Spatial patterns in phytoplankton growth and microzooplankton grazing in the Arabian Sea during monsoon forcing. Deep-Sea Research II 45, 2353–2368.

Latasa, M., Bidigare, R.R., 1998. A comparison of phytoplankton populations of the Arabian Sea during the Spring Intermonsoon and the Southwest Monsoon of 1995 as described by HPLC-analyzed pigments. Deep-Sea Research 45, 2133–2170.

Lee, C.M., Jones, B.H., Brink, K.H., Fischer, A.S., 2000. The upper-ocean response to monsoonal forcing in the Arabian Sea: seasonal and spatial variability. Deep-Sea Research II 47, 1177–1226.

Li, W.K.W., 1986. Experimental approaches to field measurements: methods and interpretation. Canadian Bulletin of Fisheries and Aquatic Sciences 214, 251–286.

Li, W.K.W., Wood, A.M., 1988. Vertical distribution of North Atlantic ultraphytoplankton: analysis by flow cytometry and epifluorescence microscopy. Deep-Sea Research 35, 1615–1638.

Lindell, D., Post, A.F., 1995. Ultraphytoplankton succession is triggered by deep winter mixing in the Gulf of Aqaba (Eilat), Red Sea. Limnology and Oceanography 40, 1130–1141.

Liu, H., Campbell, L., Landry, M.R., Nolla, H.A., Brown, S.L., Constantinou, J., 1998. *Prochlorococcus* and *Synechococcus* growth rates and contributions to production in the Arabian Sea during the 1995 Southwest and Northeast Monsoons. Deep-Sea Research II 45, 2327–2352.

McDuff, R.E., Chisholm, S.W., 1982. The calculation of in situ growth rates of phytoplankton populations from fractions of cells undergoing mitosis: a clarification. Limnology and Oceanography 27, 783–788.

Monger, B.C., Landry, M.R., 1990. Direct-interception feeding by marine zooflagellates: the importance of surface and hydrodynamic forces. Marine Ecology Progress Series 65, 123–140.

Monger, B.C., Landry, M.R., 1991. Prey-size dependency of grazing by free-living marine flagellates. Marine Ecology Progress Series 74, 239–248.

Morel, A., 1997. Consequences of a *Synechococcus* bloom upon the optical properties of oceanic (case 1) waters. Limnology and Oceanography 42, 1746–1754.

Pichard, S.L., Campbell, L., Kang, J.B., Tabita, F.R., Paul, J.H., 1996. Regulation of ribulose bisphosphate carboxylase gene expression in natural phytoplankton communities. I. Diel rhythms. Marine Ecology Progress Series 139, 257–265.

Pick, F.R., Bérubé, C., 1992. Diel cycles in the frequency of dividing cells of freshwater picocyanobacteria. Journal of Plankton Research 14, 1193–1198.

Reckermann, M., Veldhuis, M.J.W., 1997. Trophic interactions between picophytoplankton and micro- and nanozooplankton in the western Arabian Sea during the NE monsoon 1993. Aquatic Microbial Ecology 12, 263–273.

Shalapyonok, A., Olson, R.J., Shalapyonok, L.S., 1998. Ultradian growth in *Prochlorococcus* spp. Applied and Environmental Microbiology 64, 1066–1069.

Sherry, N.S., 1995. Picocyanobacteria in the Arabian Sea during the end of the winter monsoon: diurnal patterns, spatial variability, and division rates. M.S. Thesis. University of Oregon.

Sweeney, B.M., Borgese, M.B., 1989. A circadian rhythm in cell division in a prokaryote, the cyanobacterium *Synechococcus* WH7803. Journal of Phycology 25, 183–186.

Tarran, G.A., Burkill, P.H., Edwards, E.S., Woodward, E.M.S., 1999. Phytoplankton community structure in the Arabian Sea during and after the SW Monsoon, 1994. Deep-Sea Research II 46, 655–676.

Toon, R.K., Lohrenz, S.E., Rathbun, C.E., Wood, A.M., Arnone, R.A., Jones, B.H., Kindle, J.C., Weidemann, A.D., 2000. Photosynthesis-irradiance parameters and community structure associated with coastal filaments and adjacent waters in the northern Arabian Sea. Deep-Sea Research II 47, 1249–1277.

Vaulot, D., LeBot, N., Marie, D., Fukai, E., 1996. Effect of phosphorus on the *Synechococcus* cell cycle in surface mediterranean waters during summer. Applied and Environmental Microbiology 62, 2527–2533.

Veldhuis, M.J.W., Kraay, G.W., Van Bleijswijk, J.D.L., Baars, M.A., 1997. Seasonal and spatial variability in phytoplankton biomass, productivity and growth in the northwestern Indian Ocean: the southwest and northeast monsoon, 1992–1993. Deep-Sea Research I 44, 425–449.

Waterbury, J.B., Ripka, R., 1989. Subsection I. Chroococales Wettstein 1924, Emend. Rippka et al., 1979. In Staley, J.T., Bryant, M.P., Pfennig, N., Holt, J.G. (Eds.), Bergey's Manual of Systematic Bacteriology, Vol. 3, pp. 1728–1746.

Waterbury, J.B., Watson, S.W., Valois, F.W., Kranks, D.G., 1986. Biological and ecological characterization of the marine unicellular cyanobacterium *Synechococcus*. Canadian Bulletin of Fisheries and Aquatic Sciences 214, 71–120.

Wood, A.M., Lipsen, M., Coble, P., 1999. Fluorescence-based characterization of phycoerythrin-containing cyanobacterial communities in the Arabian Sea during the Northeast and early Southwest Monsoon (1994–1995). Deep-Sea Research II 46, 1769–1790.

Wyman, M., 1999. Diel rhythms in ribulose-1,5-bisphosphate carboxylase/oxygenase and glutamine synthetase gene expression in a natural population of marine picoplanktonic cyanobacteria (*Synechococcus* spp.). Applied and Environmental Microbiology 65, 3651–3659.